

Scalable Bilevel Loss Balancing for Multi-Task Learning

Peiyao Xiao* Chaosheng Dong† Shaofeng Zou‡ Kaiyi Ji§

February 13, 2025

Abstract

Multi-task learning (MTL) has been widely adopted for its ability to simultaneously learn multiple tasks. While existing gradient manipulation methods often yield more balanced solutions than simple scalarization-based approaches, they typically incur a significant computational overhead of $\mathcal{O}(K)$ in both time and memory, where K is the number of tasks. In this paper, we propose BiLB4MTL, a simple and scalable loss balancing approach for MTL, formulated from a novel bilevel optimization perspective. Our method incorporates three key components: (i) an initial loss normalization, (ii) a bilevel loss-balancing formulation, and (iii) a scalable first-order algorithm that requires only $\mathcal{O}(1)$ time and memory. Theoretically, we prove that BiLB4MTL guarantees convergence not only to a stationary point of the bilevel loss balancing problem but also to an ϵ -accurate Pareto stationary point for all K loss functions under mild conditions. Extensive experiments on diverse multi-task datasets demonstrate that BiLB4MTL achieves state-of-the-art performance in both accuracy and efficiency. Code is available at <https://github.com/OptMN-Lab/-BiLB4MTL>.

1 Introduction

In recent years, Multi-Task Learning (MTL) has received increasing attention for its ability to predict multiple tasks simultaneously using a single model, thereby reducing computational overhead. This versatility has enabled a wide range of applications, including autonomous driving (Chen et al., 2018), recommendation systems (Wang et al., 2020), and natural language processing (Zhang et al., 2022).

Typically, research in MTL follows two main schemes. *Scalarization-based* methods, such as linear scalarization, reduce MTL to a scalar optimization problem by using an averaged or weighted sum of loss functions as the objective. Due to its simplicity and scalability, it became the prominent approach in the early studies (Caruana, 1997). However, it often causes performance degradation compared with single-task learning due to the gradient conflict (Yu et al., 2020; Liu et al., 2021a). Gradient conflict arises from two main reasons: 1) gradients point in different directions and 2) gradient magnitudes vary significantly. As a result, the final update gradient may either be offset or dominated by the largest gradient (Liu et al., 2021b). To mitigate this issue, various *gradient manipulation* methods have been developed to find balanced and fair solutions via seeking a better conflict-aware update direction (Désidéri, 2012; Liu et al., 2021a; Ban & Ji,

*Peiyao Xiao and Kaiyi Ji are with the Department of Computer Science and Engineering, University at Buffalo, Buffalo, NY 14228 USA (e-mail: peiyaoxi@buffalo.edu, kaiyiji@buffalo.edu).

†Chaosheng Dong is with Amazon.com Inc, Seattle, WA, 98109 USA (e-mail: chaosd@amazon.com).

‡Shaofeng Zou is with the School of Electrical, Computer and Energy Engineering, Arizona State University, Tempe, AZ 85281 USA (e-mail: zou@asu.edu).

§Correspondence to: Kaiyi Ji (kaiyiji@buffalo.edu)

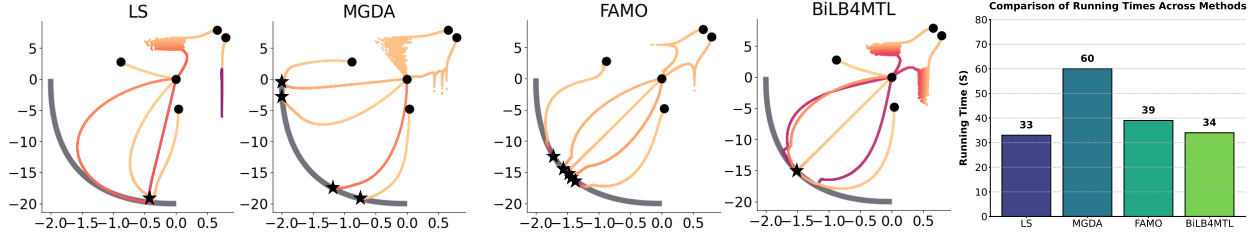


Figure 1: The loss trajectories of a toy 2-task learning problem from Liu et al. 2024 and the runtime comparison of different MTL methods for 50000 steps. Stars on the Pareto front denote the converge points. Although FAMO achieves more balanced results than LS and MGDA, it converges to different points on the Pareto front. Our method reaches the same balanced point with a computational cost comparable to the simple Linear Scalarization (LS). Full experimental details can be found in Appendix A.1.

2024; Navon et al., 2022; Yu et al., 2020; Fernando et al., 2023; Xiao et al., 2024). Nevertheless, most of these methods require computing and storing the gradients for all K tasks, resulting in substantial $O(K)$ time and memory costs. This limitation reduces their scalability in large-scale MTL applications involving complex models and extensive datasets.

In this paper, we propose a simple and scalable loss balancing approach for MTL from a novel bilevel optimization perspective. Our approach comprises three key components: initial loss normalization, a bilevel loss balancing formulation, and a scalable first-order algorithmic design. Our specific contributions are summarized as follows.

- **Bilevel loss balancing.** At the core of our bilevel formulation, the lower-level problem optimizes the model parameters by minimizing a weighted sum of normalized individual loss functions. Meanwhile, the upper-level problem adjusts these weights to minimize the disparities among the loss functions, ensuring balanced learning across tasks.
- **Scalable algorithms with $O(1)$ time and memory cost.** We develop Bilevel Loss Balancing for Multi-Task Learning (BiLB4MTL), a highly efficient algorithm tailored to solve the proposed bilevel loss balancing problem. Unlike traditional bilevel methods, BiLB4MTL has a fully single-loop structure without any second-order gradient computation, resulting in an overall $O(1)$ time and memory complexity. The 2-task toy example in Figure 1 illustrates that our BiLB4MTL method achieves a more balanced solution compared to other competitive approaches while maintaining superior computational efficiency.
- **Superior empirical performance.** Extensive experiments demonstrate that our proposed BiLB4MTL method achieves state-of-the-art performance compared to various scalarization-based and gradient manipulation methods across multiple supervised multi-task datasets, including QM9 (Ramakrishnan et al., 2014), CelebA (Liu et al., 2015), and Cityscapes (Cordts et al., 2016). Moreover, BiLB4MTL stands out as one of the most efficient and scalable methods.
- **Theoretical guarantees.** Theoretically, we show that BiLB4MTL guarantees convergence not only to a stationary point of the bilevel loss balancing problem but also to an ϵ -accurate Pareto stationary point for all K individual loss functions.

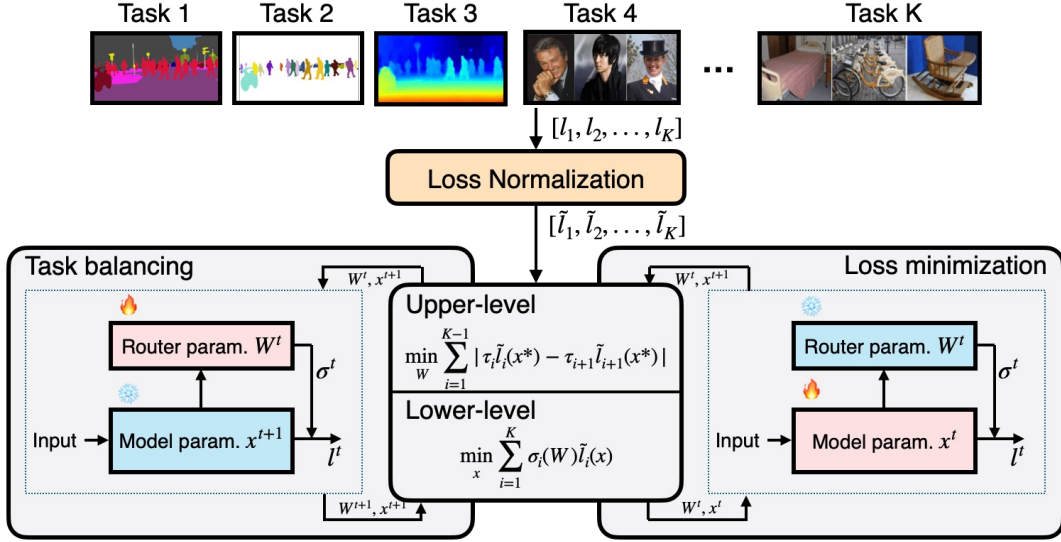


Figure 2: Our bilevel loss balancing pipeline for multi-task learning. First, task losses will be normalized through an initial loss normalization module. Then, the lower-level problem optimizes the model parameter x^t by minimizing the weighted sum of task losses and the upper-level problem optimizes the router model parameter W^t for task balancing.

2 Related Works

Multi-task learning. MTL has recently garnered significant attention in practical applications. One line of research focuses on model architecture, specifically designing various sharing mechanisms (Kokkinos, 2017; Ruder et al., 2019). Another direction addresses the mismatch in loss magnitudes across tasks, proposing methods to balance them. For example, Kendall et al. 2018 balanced tasks by weighting loss functions based on homoscedastic uncertainties, while Liu et al. 2019 dynamically adjusted weights by considering the rate of change in loss values for each task.

Besides, one prominent approach frames MTL as a Multi-Objective Optimization (MOO) problem. Sener & Koltun 2018 introduced this perspective in deep learning, inspiring methods based on the Multi-Gradient Descent Algorithm (MGDA) (Désidéri, 2012). Subsequent work has aimed to address gradient conflicts. For instance, PCGrad (Yu et al., 2020) resolves conflicts by projecting gradients onto the normal plane, GradDrop (Chen et al., 2020) randomly drops conflicting gradients, and CAGrad (Liu et al., 2021a) constrains update directions to balance gradients. Additionally, Nash-MTL (Navon et al., 2022) formulates MTL as a bargaining game among tasks, while FairGrad (Ban & Ji, 2024) incorporates α -fairness into gradient adjustments.

On the theoretical side, Zhou et al. 2022 analyzed the convergence properties of stochastic MGDA, and Fernando et al. 2023 proposed a method to reduce bias in the stochastic MGDA with theoretical guarantees. More recent advancements include a double-sampling strategy with provable guarantees introduced by Xiao et al. 2024 and Chen et al. 2024, where the latter one analyzes stochastic MOO algorithms, addressing optimization, generalization, and conflict mitigation trade-offs. Furthermore, Zhang et al. 2024 studied the convergence analysis of both deterministic and stochastic MGDA under a more relaxed generalized smoothness assumption.

Bilevel optimization. Bilevel optimization, first introduced by Bracken & McGill 1973, has been extensively studied over the past few decades. Early research primarily treated it as a constrained optimization problem

(Hansen et al., 1992; Shi et al., 2005). More recently, gradient-based methods have gained prominence due to their effectiveness in machine learning applications. Many of these approaches approximate the hypergradient using either linear systems (Domke, 2012; Ji et al., 2021) or automatic differentiation techniques (Maclaurin et al., 2015; Franceschi et al., 2017). However, these methods become impractical in large-scale settings due to their significant computational cost (Xiao & Ji, 2023; Yang et al., 2024b). The primary challenge lies in the high cost of gradient computation: approximating the Hessian-inverse vector requires multiple first- and second-order gradient evaluations, and the nested sub-loops exacerbate this inefficiency. To address these limitations, recent studies have focused on reducing the computational burden of second-order gradients. For example, some methods reformulate the lower-level problem using value-function-based constraints and solve the corresponding Lagrangian formulation (Kwon et al., 2023; Yang et al., 2024a). The work studies convex bilevel problems and proposes a zeroth-order optimization method with finite-time convergence to the Goldstein stationary point (Chen et al., 2023). In this work, we propose a simplified first-order bilevel method for MTL, motivated by intriguing empirical findings.

3 Preliminary

Scalarization-based methods. Multi-task learning (MTL) aims to optimize multiple tasks (objectives) simultaneously with a single model. The straightforward approach is to optimize a weighted summation of all loss functions:

$$\min_x L_{total}(x) = \sum_{i=1}^K w_i l_i(x),$$

where $x \in \mathbb{R}^d$ denotes the model parameter, $l_i(x) : \mathbb{R}^d \rightarrow \mathbb{R}_{\geq 0}$ represents the loss function of the i -th task and K is the number of tasks. This approach faces two key challenges: 1) fixed weights can lead to significant gradient conflicts, potentially allowing one task to dominate the learning process (Xiao et al., 2024; Wang et al., 2024); and 2) the overall performance is highly sensitive to the weighting of different losses (Kendall et al., 2018). Consequently, such methods often struggle with performance imbalances across tasks.

Gradient manipulation methods. To mitigate gradient conflicts, gradient manipulation methods dynamically compute an update d^t at each epoch to balance progress across tasks, where t is the epoch index. The update d^t is typically a convex combination of task gradients, expressed as:

$$d^t = G(x^t)w^t, \quad \text{where } w^t = h(G(x^t)),$$

with $G(x^t) = [\nabla l_1(x^t), \nabla l_2(x^t), \dots, \nabla l_K(x^t)]$. The weight vector w^t is determined by a function $h(\cdot) : \mathbb{R}^{K \times d} \rightarrow \mathbb{R}^K$, which varies depending on the specific method. However, these methods often require computing and storing the gradients of all K tasks during each epoch, making them less scalable and resource-intensive, particularly in large-scale scenarios. Therefore, it is highly demanding to develop lightweight methods that achieve balanced performance.

Pareto concepts. Solving the MTL problem is challenging because it is difficult to identify a common x that achieves the optima for all tasks. Instead, a widely accepted target is finding a Pareto stationary point. Suppose we have two points x_1 and x_2 . It is claimed that x_1 dominates x_2 if $l_i(x_1) \leq l_i(x_2) \forall i \in [K]$, and $\exists j l_j(x_1) < l_j(x_2)$. A point is Pareto optimal if it is not dominated by any other points, implying that no task can be improved further without sacrificing another. Besides, a point x is a Pareto stationary point if $\min_{w \in \mathcal{W}} \|G(x)w\| = 0$.

4 Bilevel Loss Balancing for Multi-Task Learning

In this section, we present our bilevel loss balancing framework for multi-task learning. As illustrated in Figure 2, this framework contains an initial loss normalization module, a bilevel loss balancing procedure, and a simplified first-order optimization design.

4.1 Initial loss normalization

Before applying loss balancing, an initial loss normalization step is introduced to ensure that the rescaled loss functions are on a similar and comparable scale. This step is necessary because training often involves tasks of different types (e.g., classification and regression) with distinct loss functions, as well as targets measured in varying units or scales (e.g., meters, centimeters, or millimeters). Here, we present three effective approaches that work well in different scenarios.

Identical normalization. This approach maintains the original loss values, where $\tilde{l}_i = l_i, \forall i \in [K]$. It is commonly used in multi-task classification scenarios where the loss functions of all tasks are on a similar scale, such as *cross-entropy* functions in classification problems.

Rescaled normalization. This method normalizes loss values by rescaling each task’s loss using its initial loss value l'_i , such that $\tilde{l}_i = \frac{l_i}{l'_i}$. The resulting normalized loss reflects the training progress and ensures comparability across tasks. This approach is particularly well-suited for scenarios where the loss scales do not differ significantly.

Logarithmic normalization. In some cases, the loss can vary significantly in scale. For example, as shown in Figure 3, we observed that the loss values during training across 9 regression tasks in the QM9 dataset exhibit substantial differences in magnitude, with loss ratios exceeding 1000 in certain instances. To address this issue, we propose logarithmically rescaling the loss functions such that $\tilde{l}_i = \log\left(\frac{l_i}{l_{i,0}}\right)$, where $l_{i,0}$ represents the initial loss value for the i -th task at each epoch. Our experiments demonstrate that this initialization approach stabilizes training by reducing large fluctuations caused by significant scale variations.

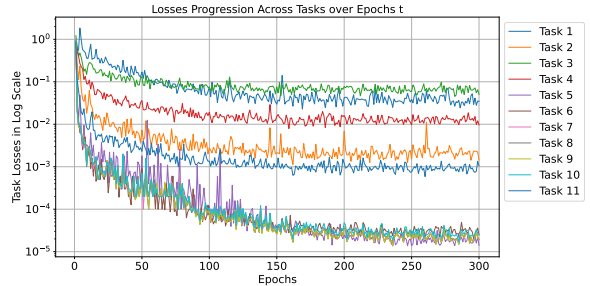


Figure 3: Curves of loss values during the training process for all 11 tasks on the QM9 dataset. The loss values vary significantly across different tasks.

4.2 Bilevel loss balancing formulation

Building on the normalized loss function values, we introduce a novel bilevel loss balancing approach for MTL to achieve a more balanced and fair solution. The formulation is as follows:

$$\begin{aligned}
 & \min_W \sum_{i=1}^{K-1} |\tau_i \tilde{l}_i(x^*) - \tau_{i+1} \tilde{l}_{i+1}(x^*)| := f(W, x^*) \\
 & \text{s.t. } x^* \in \arg \min_x \sum_{i=1}^K \sigma_i(W) \tilde{l}_i(x) := g(W, x),
 \end{aligned} \tag{1}$$

where we denote $x^* = x^*(W)$ for notational convenience. It can be seen from eq. (1) that The lower-level problem minimizes the weighted sum of losses w.r.t. the model parameters x , while the upper-level problem minimizes the accumulated weighted loss gaps w.r.t. the parameters W , ensuring balance across different tasks. Note that we define a routing function $\sigma(W) \in \mathbb{R}^K$, which is parameterized by a small neural network with a softmax output layer. For the upper-level weight vector $\tau = (\tau_1, \dots, \tau_K)$, we provide two effective options: (i) $\tau = \sigma(W)$ and (ii) $\tau = \mathbf{1}$ that work well in the experiments.

4.3 Scalable first-order algorithm design

To enable large-scale applications, we adopt an efficient and scalable first-order method to solve the problem in Equation (1). Inspired by recent advancements in first-order bilevel optimization (Kwon et al., 2023; Yang et al., 2023), we reformulate the original bilevel problem into an equivalent constrained optimization problem as follows.

$$\min_W f(W, x) \quad \text{s.t.} \quad \underbrace{\sum_{i=1}^K \sigma_i(W) \tilde{l}_i(x) - \sum_{i=1}^K \sigma_i(W) \tilde{l}_i(x^*)}_{\text{penalty function } p(W, x)} \leq 0.$$

Then, given a penalty constant $\lambda > 0$, penalizing $p(W, x)$ into the upper-level loss function yields

$$\min_{W, x} f(W, x) + \lambda \sum_{i=1}^K (\sigma_i(W) \tilde{l}_i(x) - \sigma_i(W) \tilde{l}_i(x^*)). \quad (2)$$

Intuitively, a larger λ allows more precise training on model parameters x such that x converges closer to x^* . Conversely, a smaller λ prioritizes upper-level loss balancing during training. The main challenge of solving the penalized problem above lies in the updates of W , as shown below:

$$W^{t+1} = W^t - \alpha (\nabla_W f(W^t, x^t) + \lambda (\nabla_W g(W^t, x^t) - \nabla_W g(W^t, z_N^t))), \quad (3)$$

where t is the epoch index, α is the step size, and z_N^t is an approximation of $x_t^* \in \arg \min_x g(W^t, x)$ through the following loop of N iterations each epoch.

$$z_{n+1}^t = z_n^t - \beta \nabla_z g(W^t, z_n^t), n = 0, 1, \dots, N - 1, \quad (4)$$

where N is typically chosen to be sufficiently large, ensuring that z_N^t closely approximates x_t^* (full algorithm is provided in Algorithm 2 in the appendix). Consequently, this sub-loop of iterations incurs significant computational overhead, driven by the high dimensionality of z (matching that of the model parameters) and the large value of N .

Interestingly, our experiments reveal that the gradient norm $\|\nabla_W g(W^t, z_N^t)\|$ remains sufficiently small, typically orders of magnitude smaller than the gradient norm $\|\nabla_W g(W^t, x^t)\|$, which is used to update outer parameters W . This behavior is illustrated in Figure 4. Specifically, we set $N = 50$ during training. On average, the ratio $\|\nabla_W g(W^t, x^t)\| / \|\nabla_W g(W^t, z_N^t)\|$ exceeds 100, despite some fluctuations. Under these conditions, the term $\nabla_W g(W, z_N^t)$ can be safely neglected, thereby eliminating the need for the expensive loop

Algorithm 1 BiLB4MTL

- 1: **Initialize:** W^0, x^0
 - 2: **for** $t = 0, 1, \dots, T - 1$ **do**
 - 3: $x^{t+1} = x^t - \alpha(\nabla_x f(W^t, x^t) + \lambda \nabla_x g(W^t, x^t)).$
 - 4: $W^{t+1} = W^t - \alpha(\nabla_W f(W^t, x^t) + \lambda \nabla_W g(W^t, x^t))$
 - 5: **end for**
-

in Equation (4). This approximation has been effectively utilized in large-scale applications, such as fine-tuning large language models, to reduce memory and computational costs (Shen et al., 2024a). It also serves as a foundation for our proposed algorithm, Bilevel Loss Balancing for Multi-Task Learning (BiLB4MTL), described in Algorithm 1. BiLB4MTL employs a fully single-loop structure, requiring only a single gradient computation for both variables per epoch, resulting in an $\mathcal{O}(1)$ time and memory cost.

In Section 6, we show that our BiLB4MTL method attains both an ϵ -accurate stationary point for the bilevel problem in eq. (1) and an ϵ -accurate Pareto stationary point for original loss functions under mild conditions.

5 Empirical Results

In this section, we conduct extensive practical experiments under multi-task classification, regression, and mixed settings to demonstrate the effectiveness of our method. Full experimental details can be found in Appendix A.

Baselines and evaluation. To demonstrate the effectiveness of our proposed method, we evaluate its performance against a broad range of baseline approaches. The compared methods include scalarization-based algorithms, such as Linear Scalarization (LS), Scale-Invariant (SI), Random Loss Weighting (RLW) (Lin et al., 2021), Dynamic Weight Average (DWA) (Liu et al., 2019), and Uncertainty Weighting (UW) (Kendall et al., 2018), GO4Align (Shen et al., 2024b). We also benchmark against gradient manipulation methods, including Multi-Gradient Descent Algorithm (MGDA) (Désidéri, 2012), PCGrad (Yu et al., 2020), GradDrop (Chen et al., 2020), CAGrad (Liu et al., 2021a), IMTL-G (Liu et al., 2021b), Nash-MTL (Navon et al., 2022), FAMO (Liu et al., 2024), and FairGrad (Ban & Ji, 2024). To provide a comprehensive evaluation, we report the performance of each individual task and employ one additional metric: $\Delta m\%$ to quantify overall performance. The $\Delta m\%$ metric measures the average relative performance drop of a multi-task model compared to its corresponding single-task baseline. Formally, it is defined as:

$$\Delta m\% = \frac{1}{K} \sum_{i=1}^K (-1)^{\delta_k} (M_{m,k} - M_{b,k}) / M_{b,k} \times 100,$$

where $M_{m,k}$ and $M_{b,k}$ represent the performance of the k -th task for the multi-task model m and single-task model b , respectively. The indicator $\delta_k = 1$ if lower values indicate better performance and 0 otherwise.

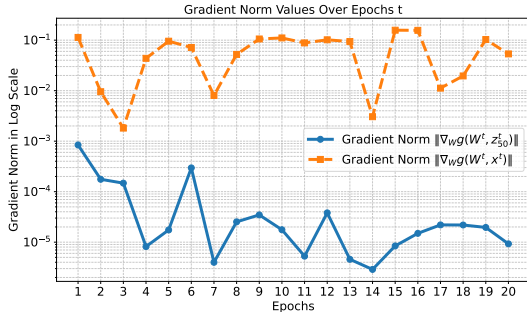


Figure 4: Gradient norm values during the training process on the Cityscapes dataset. Similar phenomena have also been observed in other datasets.

Table 1: Results on Cityscapes (2-task) dataset. Each experiment is repeated 3 times with different random seeds and the average is reported. The best results are highlighted in **bold**, while the second-best results are indicated with underlines.

METHOD	SEGMENTATION		DEPTH		$\Delta m\% \downarrow$
	MIOU \uparrow	PIX ACC \uparrow	ABS ERR \downarrow	REL ERR \downarrow	
STL	74.01	93.16	0.0125	27.77	
LS	75.18	93.49	0.0155	46.77	22.60
SI	70.95	91.73	0.0161	33.83	14.11
RLW	74.57	93.41	0.0158	47.79	24.38
DWA	75.24	93.52	0.0160	44.37	21.45
UW	72.02	92.85	0.0140	30.13	5.89
FAMO	74.54	93.29	0.0145	32.59	8.13
GO4ALIGN	72.63	93.03	0.0164	<u>27.58</u>	8.11
MGDA	68.84	91.54	0.0309	33.50	44.14
PCGRAD	75.13	93.48	0.0154	42.07	18.29
GRADDROP	75.27	93.53	0.0157	47.54	23.73
CAGRAD	75.16	93.48	0.0141	37.60	11.64
IMTL-G	75.33	93.49	0.0135	38.41	11.10
MoCo	<u>75.42</u>	93.55	0.0149	34.19	9.90
NASH-MTL	75.41	<u>93.66</u>	0.0129	35.02	6.82
FAIRGRAD	75.72	93.68	0.0134	32.25	5.18
BiLB4MTL ($\tau = 1$)	74.53	93.42	<u>0.0128</u>	26.79	-0.57
BiLB4MTL ($\tau = \sigma$)	74.92	93.24	0.0127	29.80	<u>1.93</u>

5.1 Experiment setup

Here, we summarize our experimental setup, including the dataset, configuration, and hyperparameter tuning.

Image-Level Classification. CelebA (Liu et al., 2015), one of the most widely used datasets, is a large-scale facial attribute dataset containing over 200K celebrity images. Each image is annotated with 40 attributes, such as the presence of eyeglasses and smiling. Following the experimental setup in Ban & Ji 2024, we treat CelebA as a 40-task multi-task learning (MTL) classification problem, where each task predicts the presence of a specific attribute. Since all tasks involve binary classification with the same *binary cross-entropy* loss function, we apply identical normalization for both options of $\tau = 1$ and $\tau = \sigma$ at the initial loss normalization stage. The network architecture consists of a 9-layer convolutional neural network (CNN) as the shared model, with multiple linear layers serving as task-specific heads. We train the model for 15 epochs using the Adam optimizer with a batch size of 256.

Regression. QM9 (Ramakrishnan et al., 2014) dataset is another widely used benchmark for multi-task regression problems in quantum chemistry. It contains 130K molecules represented as graphs, and 11 properties to be predicted. Though all tasks share the same loss function, *mean squared error*, they exhibit varying scales: a phenomenon commonly observed in regression tasks but less prevalent in classification tasks, as shown in Figure 3. To address this scale discrepancy, we adopt the logarithmic normalization in Section 4.1 at the initial loss normalization stage for both options of $\tau = 1$ and $\tau = \sigma$. Following the experimental setup

Table 2: Results on CelebA (40-task) and NYU-v2 (3-task) datasets. Each experiment is repeated 3 times and the average is reported. The best results are highlighted in **bold**, while the second-best results are indicated with underlines.

METHOD	CELEBA (40 TASKS)	NYU-v2 (3 TASKS)
	$\Delta m\% \downarrow$	$\Delta m\% \downarrow$
LS	4.15	5.59
SI	7.20	4.39
RLW	1.46	7.78
DWA	3.20	3.57
UW	3.23	4.05
FAMO	1.21	-4.10
GO4ALIGN	0.88	-6.08
MGDA	14.85	1.38
PCGRAD	3.17	3.97
CAGRAD	2.48	0.20
IMTL-G	0.84	-0.76
NASH-MTL	2.84	-4.04
FAIRGRAD	0.37	<u>-4.66</u>
BiLB4MTL ($\tau = 1$)	<u>-1.07</u>	-4.40
BiLB4MTL ($\tau = \sigma$)	-1.31	-3.52

in Liu et al. 2024; Navon et al. 2022, we use the same model and data split, 110K molecules for training, 10k for validation, and the rest 10k for testing. The model is trained 300 epochs with a batch size of 120. The learning rate starts at 1e-3 and is reduced whenever the validation performance stagnates for 5 consecutive epochs.

Dense Prediction. The Cityscapes dataset (Cordts et al., 2016) consists of 5000 street-scene images designed for two tasks: 7-class semantic segmentation (a classification task) and depth estimation (a regression task). Similarly, the NYU-v2 dataset (Silberman et al., 2012) is widely used for indoor scene understanding and contains 1449 densely annotated images. It includes one pixel-level classification task, semantic segmentation, and two pixel-level regression tasks, 13-class depth estimation plus surface normal prediction. These datasets provide benchmarks for evaluating the performance of our method in mixed multi-task settings. Since the number of tasks is small and the loss values exhibit minimal variation, we applied rescaled normalization when selecting $\tau = \sigma$ and identical normalization when selecting $\tau = 1$. We follow the same experimental setup described in Liu et al. 2021a; Navon et al. 2022 and adopt MTAN (Liu et al., 2019) as the backbone, which incorporates task-specific attention modules into SegNet (Badrinarayanan et al., 2017). Both models are trained for 200 epochs, with batch sizes of 8 for Cityscapes and 8 for NYU-v2. The learning rates are initialized at 3e-4 and 1e-4 for the first 100 epochs and reduced by half for the remaining epochs, respectively.

Hyperparameter tuning. In our method, hyperparameters include the step size α and the penalty constant λ . For the step size, we adopt the settings from prior experiments without extensive tuning. While we use the same step size for updates to both W and x in our implementation, these can be adjusted independently in practice. For λ , we determine the optimal value through a grid search. Starting with a coarse range $\lambda \in [0.01, 0.1, 1, 2, 5, 10]$, we evaluate performance and determine which value is better. Then we narrow

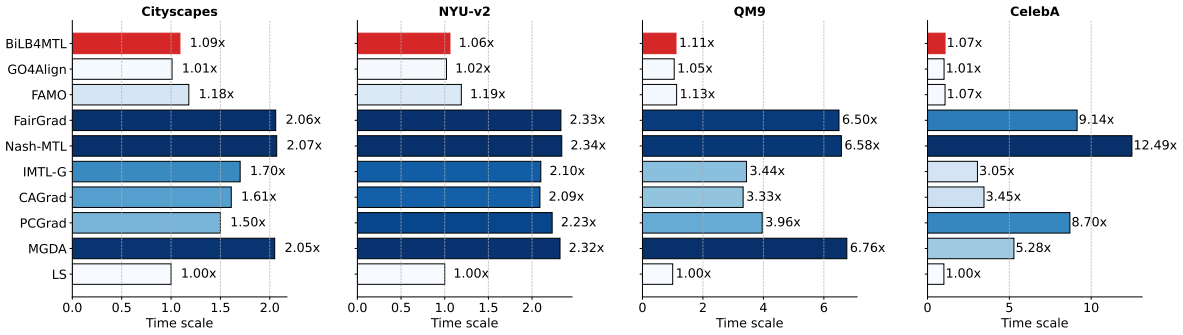


Figure 5: Time scale comparison among well-performing approaches, with LS considered the reference method for standard time.

down the search space and continue to execute a finer grid search with a step size of 0.1 or 0.02 until we determine an appropriate value.

5.2 Experimental results

Results on the four benchmark datasets are provided in Table 1, Table 2, and Table 3. We observe that BiLB4MTL outperforms existing methods on both the CelebA and QM9 datasets, achieving the lowest performance drops of $\Delta m\% = -1.31$ and $\Delta m\% = 49.5$, respectively. Detailed results for the QM9 dataset illustrate that it achieves a balanced performance across all tasks. Besides, the BiLB4MTL($\tau = 1$) does not effectively minimize task disparities due to large loss scale differences. These results highlight the effectiveness of our method in handling a large number of tasks in both classification and regression settings. Meanwhile, it achieves the lowest performance drop, with $\Delta m\% = -0.57$ on the Cityscapes dataset, while delivering comparable results on the NYU-v2 dataset, where the detailed results are shown in Table 4 in the Appendix. These findings highlight the capability of BiLB4MTL to effectively handle mixed multi-task learning scenarios.

Additionally, we conducted an ablation study to evaluate the impact of different normalization strategies. The results, presented in Table 5 in the Appendix, demonstrate the effectiveness of our proposed normalization methods.

5.3 MTL efficiency

Finally, we compare the running times of well-performing approaches in Figure 5. Notably, our BiLB4MTL introduces negligible overhead compared with LS with at most a $1.11\times$ increase, aligning with other $\mathcal{O}(1)$ methods such as GO4Align and FAMO. In contrast, gradient manipulation methods, taking $\mathcal{O}(K)$ computational cost, become significantly slower in many-task scenarios. For example, Nash-MTL requires approximately $12\times$ times more than BiLB4MTL on the CelebA dataset.

6 Theoretical Analysis

In this section, we provide convergence analysis for our BiLB4MTL method. We first provide several useful definitions and assumptions.

Table 3: Detailed results of on QM9 (11-task) dataset. Each experiment is repeated 3 times and the average is reported. The best results are highlighted in **bold**, while the second-best results are indicated with underlines.

METHOD	μ	α	ϵ_{HOMO}	ϵ_{LUMO}	$\langle R^2 \rangle$	ZPVE	U_0	U	H	G	c_v	$\Delta m\% \downarrow$
MAE \downarrow												
STL	0.067	0.181	60.57	53.91	0.502	4.53	58.8	64.2	63.8	66.2	0.072	
LS	0.106	0.325	73.57	89.67	5.19	14.06	143.4	144.2	144.6	140.3	0.128	177.6
SI	0.309	0.345	149.8	135.7	<u>1.00</u>	<u>4.50</u>	55.3	55.75	55.82	55.27	0.112	77.8
RLW	0.113	0.340	76.95	92.76	5.86	15.46	156.3	157.1	157.6	153.0	0.137	203.8
DWA	0.107	0.325	<u>74.06</u>	90.61	5.09	13.99	142.3	143.0	143.4	139.3	0.125	175.3
UW	0.386	0.425	166.2	155.8	1.06	4.99	66.4	66.78	66.80	66.24	0.122	108.0
FAMO	0.15	0.30	94.0	95.2	1.63	4.95	70.82	71.2	71.2	70.3	0.10	58.5
GO4ALIGN	0.17	0.35	102.4	119.0	1.22	4.94	<u>53.9</u>	<u>54.3</u>	<u>54.3</u>	<u>53.9</u>	0.11	<u>52.7</u>
MGDA	0.217	0.368	126.8	104.6	3.22	5.69	88.37	89.4	89.32	88.01	0.120	120.5
PCGRAD	<u>0.106</u>	0.293	75.85	88.33	3.94	9.15	116.36	116.8	117.2	114.5	0.110	125.7
CAGRAD	0.118	0.321	83.51	94.81	3.21	6.93	113.99	114.3	114.5	112.3	0.116	112.8
IMTL-G	0.136	0.287	98.31	93.96	1.75	5.69	101.4	102.4	102.0	100.1	0.096	77.2
NASH-MTL	0.102	0.248	82.95	81.89	2.42	5.38	74.5	75.02	75.10	74.16	0.093	62.0
FAIRGRAD	0.117	<u>0.253</u>	87.57	<u>84.00</u>	2.15	5.07	70.89	71.17	71.21	70.88	<u>0.095</u>	57.9
BiLB4MTL ($\tau = 1$)	0.341	0.405	161.49	140.06	1.65	5.04	75.31	74.82	75.66	75.82	0.125	113.6
BiLB4MTL ($\tau = \sigma$)	0.23	0.29	123.89	111.95	0.97	3.99	42.73	43.1	43.2	43.1	0.097	49.5

Definition 1. Given $L > 0$, a function ℓ is said to be L -Lipschitz-continuous on \mathcal{X} if it holds for any $x, x' \in \mathcal{X}$ that $\|\ell(x) - \ell(x')\| \leq L\|x - x'\|$. A function ℓ is said to be L -Lipschitz-smooth if its gradient is L -Lipschitz-continuous.

Definition 2 (Pareto stationarity). We say x is an ϵ -accurate Pareto stationary point for loss functions $\{l_i(x)\}$ if $\min_{w \in \mathcal{W}} \|G(x)w\|^2 = \mathcal{O}(\epsilon)$, where $G(x) = [\nabla l_1(x), \nabla l_2(x), \dots, \nabla l_K(x)]$.

Inspired by Shen & Chen 2023, we define the following two surrogates of the original bilevel problem in eq. (1), as shown below.

Definition 3. Define two surrogate bilevel problems as

$$\begin{aligned} \mathcal{BP}_\lambda &: \min_{W,x} f(W,x) + \lambda(g(W,x) - g(W,x^*)), \\ \mathcal{BP}_\epsilon &: \min_{W,x} f(W,x) \text{ s.t. } g(W,x) - g(W,x^*) \leq \epsilon, \end{aligned} \quad (5)$$

where \mathcal{BP}_λ is the penalized bilevel problem, and \mathcal{BP}_ϵ recovers to the original bilevel problem if $\epsilon = 0$.

Assumption 1 (Lipschitz and smoothness). There exists a constant L such that the upper-level function $f(W, \cdot)$ is L -Lipschitz continuous. There exists constants L_f and L_g such that functions $f(W, x)$ and $g(W, x)$ are L_f - and L_g -Lipschitz-smooth.

Assumption 2 (Polyak-Lojasiewicz (PL) condition). The lower-level function $g(W, \cdot)$ satisfies the $\frac{1}{\mu}$ -PL condition such that given any W , the following inequality holds for any feasible x .

$$\|\nabla g(W, x)\|^2 \geq \frac{1}{\mu}(g(W, x) - g(W, x^*)).$$

Lipschitz continuity and smoothness are standard assumptions in the study of bilevel optimization (Ghadimi & Wang, 2018; Ji et al., 2021). While the absolute values in the upper-level function in Equation (1) are non-smooth, they can be easily modified to ensure smoothness, such as by using a soft absolute value function of the form $y = \sqrt{x^2 + \epsilon}$ where ϵ is a small positive constant. Moreover, the PL condition can be satisfied in over-parameterized neural network settings (Mei et al., 2020; Frei & Gu, 2021). The following theorem presents the convergence analysis of our algorithms.

Theorem 1. *Suppose Assumption 1-Assumption 2 are satisfied. Select hyperparameters*

$$\alpha \in \left(0, \frac{1}{L_f + \lambda(2L_g + L_g^2\mu)}\right], \beta \in \left(0, \frac{1}{L_g}\right],$$

$$\lambda = L\sqrt{3\mu\epsilon^{-1}}, \text{ and } N = \Omega(\log(\alpha t)).$$

(i) *Our method with the updates eq. (3) and eq. (4) (i.e., Algorithm 2 in the appendix) finds an ϵ -accurate stationary point of the problem \mathcal{BP}_λ . If this stationary point is a local/global solution to \mathcal{BP}_λ , it is also a local/global solution to \mathcal{BP}_ϵ . Furthermore, it is also an ϵ -accurate Pareto stationary point for loss functions $l_i(x), i = 1, \dots, K$.*

(ii) *Moreover, if $\|\nabla_W g(W^t, z_N^t)\| = \mathcal{O}(\epsilon)$ for $t = 1, \dots, T$. The simplified method in Algorithm 1 also achieves the same convergence guarantee as that in (i) with $\mathcal{O}(\epsilon^{-2})$ iterations.*

The complete proof is provided in Theorem 2. In the first part of our theorem, we establish a connection between the stationarity of \mathcal{BP}_λ and Pareto stationarity, as well as an equivalence between the Pareto stationarities of the original loss functions $\{l_i\}$ and the normalized loss functions $\{\tilde{l}_i\}$. The second part of Theorem 1 introduces an additional gradient vanishing assumption, which has been validated in our experiments. It demonstrates that our simplified BiLB4MTL method can also attain an ϵ -accurate stationary point for the problem \mathcal{BP}_λ and an ϵ -accurate Pareto stationary point for the original loss functions.

7 Conclusion

We introduced BiLB4MTL, a scalable loss balancing approach for multi-task learning based on bilevel optimization. Our method achieves efficient loss balancing with only $\mathcal{O}(1)$ time and memory complexity while guaranteeing convergence to both a stationary point of the bilevel problem and an ϵ -accurate Pareto stationary point for all task loss functions. Extensive experiments demonstrate that BiLB4MTL outperforms existing methods in both accuracy and efficiency, highlighting its effectiveness for large-scale MTL.

For future work, we plan to explore the application of our method to broader multi-task learning problems, including recommendation systems.

Impact Statement

This paper presents work to advance the field of multi-task Learning. There are many potential societal consequences of our work, none of which we feel must be specifically highlighted here.

References

Vijay Badrinarayanan, Alex Kendall, and Roberto Cipolla. Segnet: A deep convolutional encoder-decoder architecture for image segmentation. *IEEE Transactions on Pattern Analysis and Machine Intelligence*, 39(12):2481–2495, 2017.

- Hao Ban and Kaiyi Ji. Fair resource allocation in multi-task learning. *arXiv preprint arXiv:2402.15638*, 2024.
- Jerome Bracken and James T McGill. Mathematical programs with optimization problems in the constraints. *Operations Research*, 21(1):37–44, 1973.
- Rich Caruana. Multitask learning. *Machine Learning*, 28:41–75, 1997.
- Lesi Chen, Jing Xu, and Jingzhao Zhang. Bilevel optimization without lower-level strong convexity from the hyper-objective perspective. *arXiv preprint arXiv:2301.00712*, 2023.
- Lisha Chen, Heshan Fernando, Yiming Ying, and Tianyi Chen. Three-way trade-off in multi-objective learning: Optimization, generalization and conflict-avoidance. *Advances in Neural Information Processing Systems*, 36, 2024.
- Yaran Chen, Dongbin Zhao, Le Lv, and Qichao Zhang. Multi-task learning for dangerous object detection in autonomous driving. *Information Sciences*, 432:559–571, 2018.
- Zhao Chen, Jiquan Ngiam, Yanping Huang, Thang Luong, Henrik Kretzschmar, Yuning Chai, and Dragomir Anguelov. Just pick a sign: Optimizing deep multitask models with gradient sign dropout. *Advances in Neural Information Processing Systems*, 33:2039–2050, 2020.
- Marius Cordts, Mohamed Omran, Sebastian Ramos, Timo Rehfeld, Markus Enzweiler, Rodrigo Benenson, Uwe Franke, Stefan Roth, and Bernt Schiele. The cityscapes dataset for semantic urban scene understanding. In *Proceedings of the IEEE Conference on Computer Vision and Pattern Recognition*, pp. 3213–3223, 2016.
- Jean-Antoine Désidéri. Multiple-gradient descent algorithm (mgda) for multiobjective optimization. *Comptes Rendus Mathématique*, 350(5-6):313–318, 2012.
- Justin Domke. Generic methods for optimization-based modeling. In *Artificial Intelligence and Statistics*, pp. 318–326. PMLR, 2012.
- Heshan Fernando, Han Shen, Miao Liu, Subhajit Chaudhury, Keerthiram Murugesan, and Tianyi Chen. Mitigating gradient bias in multi-objective learning: A provably convergent approach. In *International Conference on Learning Representations*, 2023.
- Luca Franceschi, Michele Donini, Paolo Frasconi, and Massimiliano Pontil. Forward and reverse gradient-based hyperparameter optimization. In *International Conference on Machine Learning*, pp. 1165–1173. PMLR, 2017.
- Spencer Frei and Quanquan Gu. Proxy convexity: A unified framework for the analysis of neural networks trained by gradient descent. *Advances in Neural Information Processing Systems*, 34:7937–7949, 2021.
- Saeed Ghadimi and Mengdi Wang. Approximation methods for bilevel programming. *arXiv preprint arXiv:1802.02246*, 2018.
- Pierre Hansen, Brigitte Jaumard, and Gilles Savard. New branch-and-bound rules for linear bilevel programming. *SIAM Journal on Scientific and Statistical Computing*, 13(5):1194–1217, 1992.

- Kaiyi Ji, Junjie Yang, and Yingbin Liang. Bilevel optimization: Convergence analysis and enhanced design. In *International Conference on Machine Learning*, pp. 4882–4892. PMLR, 2021.
- Alex Kendall, Yarin Gal, and Roberto Cipolla. Multi-task learning using uncertainty to weigh losses for scene geometry and semantics. In *Proceedings of the IEEE Conference on Computer Vision and Pattern Recognition*, pp. 7482–7491, 2018.
- Iasonas Kokkinos. Ubernet: Training a universal convolutional neural network for low-, mid-, and high-level vision using diverse datasets and limited memory. In *Proceedings of the IEEE Conference on Computer Vision and Pattern Recognition*, pp. 6129–6138, 2017.
- Jeongyeol Kwon, Dohyun Kwon, Stephen Wright, and Robert D Nowak. A fully first-order method for stochastic bilevel optimization. In *International Conference on Machine Learning*, pp. 18083–18113. PMLR, 2023.
- Baijiong Lin, Feiyang Ye, Yu Zhang, and Ivor W Tsang. Reasonable effectiveness of random weighting: A litmus test for multi-task learning. *arXiv preprint arXiv:2111.10603*, 2021.
- Bo Liu, Xingchao Liu, Xiaojie Jin, Peter Stone, and Qiang Liu. Conflict-averse gradient descent for multi-task learning. *Advances in Neural Information Processing Systems*, 34:18878–18890, 2021a.
- Bo Liu, Yihao Feng, Peter Stone, and Qiang Liu. Famo: Fast adaptive multitask optimization. *Advances in Neural Information Processing Systems*, 36, 2024.
- Liyang Liu, Yi Li, Zhanghui Kuang, J Xue, Yimin Chen, Wenming Yang, Qingmin Liao, and Wayne Zhang. Towards impartial multi-task learning. In *Proceedings of the International Conference on Learning Representations (ICLR) 2021*, 2021b.
- Shikun Liu, Edward Johns, and Andrew J Davison. End-to-end multi-task learning with attention. In *Proceedings of the IEEE/CVF Conference on Computer Vision and Pattern Recognition*, pp. 1871–1880, 2019.
- Ziwei Liu, Ping Luo, Xiaogang Wang, and Xiaoou Tang. Deep learning face attributes in the wild. In *Proceedings of the IEEE International Conference on Computer Vision*, pp. 3730–3738, 2015.
- Dougal Maclaurin, David Duvenaud, and Ryan Adams. Gradient-based hyperparameter optimization through reversible learning. In *International Conference on Machine Learning*, pp. 2113–2122. PMLR, 2015.
- Jincheng Mei, Chenjun Xiao, Csaba Szepesvari, and Dale Schuurmans. On the global convergence rates of softmax policy gradient methods. In *International Conference on Machine Learning*, pp. 6820–6829. PMLR, 2020.
- Aviv Navon, Aviv Shamsian, Idan Achituve, Haggai Maron, Kenji Kawaguchi, Gal Chechik, and Ethan Fetaya. Multi-task learning as a bargaining game. *arXiv preprint arXiv:2202.01017*, 2022.
- Raghunathan Ramakrishnan, Pavlo O Dral, Matthias Rupp, and O Anatole Von Lilienfeld. Quantum chemistry structures and properties of 134 kilo molecules. *Scientific Data*, 1(1):1–7, 2014.
- Sebastian Ruder, Joachim Bingel, Isabelle Augenstein, and Anders Søgaard. Latent multi-task architecture learning. In *Proceedings of the AAAI Conference on Artificial Intelligence*, volume 33, pp. 4822–4829, 2019.

- Ozan Sener and Vladlen Koltun. Multi-task learning as multi-objective optimization. *Advances in Neural Information Processing Systems*, 31, 2018.
- Han Shen and Tianyi Chen. On penalty-based bilevel gradient descent method. In *International Conference on Machine Learning*, pp. 30992–31015. PMLR, 2023.
- Han Shen, Pin-Yu Chen, Payel Das, and Tianyi Chen. Seal: Safety-enhanced aligned llm fine-tuning via bilevel data selection. *arXiv preprint arXiv:2410.07471*, 2024a.
- Jiayi Shen, Cheems Wang, Zehao Xiao, Nanne Van Noord, and Marcel Worring. Go4align: Group optimization for multi-task alignment. *arXiv preprint arXiv:2404.06486*, 2024b.
- Chenggen Shi, Jie Lu, and Guangquan Zhang. An extended kuhn–tucker approach for linear bilevel programming. *Applied Mathematics and Computation*, 162(1):51–63, 2005.
- Nathan Silberman, Derek Hoiem, Pushmeet Kohli, and Rob Fergus. Indoor segmentation and support inference from rgb-d images. In *Computer Vision—ECCV 2012: 12th European Conference on Computer Vision, Florence, Italy, October 7–13, 2012, Proceedings, Part V 12*, pp. 746–760. Springer, 2012.
- Menghan Wang, Yujie Lin, Guli Lin, Keping Yang, and Xiao-ming Wu. M2grl: A multi-task multi-view graph representation learning framework for web-scale recommender systems. In *Proceedings of the 26th ACM SIGKDD International Conference on Knowledge Discovery & Data Mining*, pp. 2349–2358, 2020.
- Yudan Wang, Peiyao Xiao, Hao Ban, Kaiyi Ji, and Shaofeng Zou. Finite-time analysis for conflict-avoidant multi-task reinforcement learning. *arXiv preprint arXiv:2405.16077*, 2024.
- Peiyao Xiao and Kaiyi Ji. Communication-efficient federated hypergradient computation via aggregated iterative differentiation. In *International Conference on Machine Learning*, pp. 38059–38086. PMLR, 2023.
- Peiyao Xiao, Hao Ban, and Kaiyi Ji. Direction-oriented multi-objective learning: Simple and provable stochastic algorithms. *Advances in Neural Information Processing Systems*, 36, 2024.
- Yifan Yang, Peiyao Xiao, and Kaiyi Ji. Achieving $\mathcal{O}(\epsilon^{-1.5})$ complexity in hessian/jacobian-free stochastic bilevel optimization. *arXiv preprint arXiv:2312.03807*, 2023.
- Yifan Yang, Hao Ban, Minhui Huang, Shiqian Ma, and Kaiyi Ji. Tuning-free bilevel optimization: New algorithms and convergence analysis. *arXiv preprint arXiv:2410.05140*, 2024a.
- Yifan Yang, Peiyao Xiao, and Kaiyi Ji. Simfbo: Towards simple, flexible and communication-efficient federated bilevel learning. *Advances in Neural Information Processing Systems*, 36, 2024b.
- Tianhe Yu, Saurabh Kumar, Abhishek Gupta, Sergey Levine, Karol Hausman, and Chelsea Finn. Gradient surgery for multi-task learning. *Advances in Neural Information Processing Systems*, 33:5824–5836, 2020.
- Qi Zhang, Peiyao Xiao, Kaiyi Ji, and Shaofeng Zou. On the convergence of multi-objective optimization under generalized smoothness. *arXiv preprint arXiv:2405.19440*, 2024.
- Zhihan Zhang, Wenhao Yu, Mengxia Yu, Zhichun Guo, and Meng Jiang. A survey of multi-task learning in natural language processing: Regarding task relatedness and training methods. *arXiv preprint arXiv:2204.03508*, 2022.

Shiji Zhou, Wenpeng Zhang, Jiyan Jiang, Wenliang Zhong, Jinjie Gu, and Wenwu Zhu. On the convergence of stochastic multi-objective gradient manipulation and beyond. *Advances in Neural Information Processing Systems*, 35:38103–38115, 2022.

A Experiment setup

A.1 Toy example

To better understand the benefits of our method, we illustrate the training trajectory along with the training time in a toy example of 2-task learning following the same setting in FAMO (Liu et al., 2024). The loss functions $L_1(x), L_2(x)$, where x is the model parameter, of two tasks are listed below.

$$\begin{aligned} L_1(x) &= 0.1 \times (c_1(x)f_1(x) + c_2(x)g_1(x)), \quad L_2(x) = c_1(x)f_2(x) + c_2(x)g_2(x) \quad \text{where} \\ f_1(x) &= \log(\max(|0.5(-x_1 - 7) - \tanh(-x_2)|, 0.000005)) + 6, \\ f_2(x) &= \log(\max(|0.5(-x_1 + 3) - \tanh(-x_2) + 2|, 0.000005)) + 6, \\ g_1(x) &= ((-x_1 + 7)^2 + 0.1 * (-x_2 - 8)^2)/10 - 20, \\ g_2(x) &= ((-x_1 - 7)^2 + 0.1 * (-x_2 - 8)^2)/10 - 20, \\ c_1(x) &= \max(\tanh(0.5 * x_2), 0) \quad \text{and} \quad c_2(x) = \max(\tanh(-0.5 * x_2), 0). \end{aligned} \tag{6}$$

In Figure 1, the black dots represent 5 chosen initial points $\{(-8.5, 7.5), (-8.5, 5), (0, 0), (9, 9), (10, -8)\}$ while the black stars represent the converging points on the Pareto front. We use the Adam optimizer and train each method for 50k steps. Our method can always converge to balanced results efficiently. We use Adam optimizer with a learning rate of $1e-3$. The training time is recalculated according to real-time ratios in our machine. We find that LS and MGDA do not converge to balanced points while FAMO converges to balanced results to some extent. Meanwhile, our method with rescale normalization can always converge to balanced results efficiently.

A.2 Ablation study on normalization alternatives

We conducted an ablation study on normalization strategies for the QM9 dataset, where the $\Delta m\%$ metric was computed and presented in Table 5. The best results were achieved by using a weighted sum of log-normalized losses as the lower-level objective and a weighted sum of log-normalized loss gaps as the upper-level objective. This approach aligns with our formulation in Equation (1), incorporating logarithmic normalization of loss values. In Table 5, weighted indicates the inclusion of $\sigma(W)$, log refers to the application of the logarithmic operator, and normalized signifies the division by the initial loss values.

Table 5: Ablation study on normalization alternatives.

Upper-Level \ Lower-Level	Weighted normalized loss	Weighted log-normalized loss
Weighted log-normalized loss gaps	150.3	49.5
Log-normalized loss gaps	103.9	113.6
Weighted normalized loss gaps	197.3	94.5
Normalized loss gaps	147.5	157.6
Weighted Loss gaps	125.8	72.6
Loss gaps	172.3	76.7

Table 4: Results on NYU-v2 (3-task) dataset. Each experiment is repeated 3 times with different random seeds and the average is reported.

METHOD	SEGMENTATION		DEPTH		SURFACE NORMAL					$\Delta m\% \downarrow$
	MIOU \uparrow	PIX ACC \uparrow	ABS ERR \downarrow	REL ERR \downarrow	ANGLE DISTANCE \downarrow		WITHIN $t^\circ \uparrow$			
					MEAN	MEDIAN	11.25	22.5	30	
STL	38.30	63.76	0.6754	0.2780	25.01	19.21	30.14	57.20	69.15	
LS	39.29	65.33	0.5493	0.2263	28.15	23.96	22.09	47.50	61.08	5.59
SI	38.45	64.27	0.5354	0.2201	27.60	23.37	22.53	48.57	62.32	4.39
RLW	37.17	63.77	0.5759	0.2410	28.27	24.18	22.26	47.05	60.62	7.78
DWA	39.11	65.31	0.5510	0.2285	27.61	23.18	24.17	50.18	62.39	3.57
UW	36.87	63.17	0.5446	0.2260	27.04	22.61	23.54	49.05	63.65	4.05
FAMO	38.88	64.90	0.5474	0.2194	25.06	19.57	29.21	56.61	68.98	-4.10
GO4ALIGN	40.42	65.37	0.5492	0.2167	24.76	18.94	30.54	57.87	69.84	-6.08
MGDA	30.47	59.90	0.6070	0.2555	24.88	19.45	29.18	56.88	69.36	1.38
PCGRAD	38.06	64.64	0.5550	0.2325	27.41	22.80	23.86	49.83	63.14	3.97
GRADDROP	39.39	65.12	0.5455	0.2279	27.48	22.96	23.38	49.44	62.87	3.58
CAGRAD	39.79	65.49	0.5486	0.2250	26.31	21.58	25.61	52.36	65.58	0.20
IMTL-G	39.35	65.60	0.5426	0.2256	26.02	21.19	26.20	53.13	66.24	-0.76
MoCo	40.30	66.07	0.5575	0.2135	26.67	21.83	25.61	51.78	64.85	0.16
NASH-MTL	40.13	65.93	0.5261	0.2171	25.26	20.08	28.40	55.47	68.15	-4.04
FAIRGRAD	39.74	66.01	0.5377	0.2236	24.84	19.60	29.26	56.58	69.16	-4.66
BiLB4MTL($\tau = 1$)	38.04	38.04	0.5402	0.2278	24.70	19.19	29.97	57.44	69.69	-4.40
BiLB4MTL($\tau = \sigma$)	40.94	66.21	0.5316	0.2210	25.33	20.35	27.79	54.95	67.82	-3.52

B Additional information

Here, we present the complete version of the double-loop algorithm for solving the penalized bilevel problem, \mathcal{BP}_λ in Equation (2), as detailed in Algorithm 2. Notably, the local or global solution of \mathcal{BP}_λ obtained by Algorithm 2 also serves as a local or global solution to \mathcal{BP}_ϵ , as established by Proposition 2 in Shen & Chen 2023.

C Analysis

In the analysis, we need the following definitions.

$$\begin{aligned}
 x_t^* &= \arg \min_x g(W^t, x), \quad G(x) = [\nabla l_1(x), \nabla l_2(x), \dots, \nabla l_K(x)], \quad \tilde{G}(x) = [\nabla \tilde{l}_1(x), \nabla \tilde{l}_2(x), \dots, \nabla \tilde{l}_K(x)] \\
 F(\theta^t) &= f(\theta^t) + \lambda p(\theta^t), \quad \Phi(\theta^t) = f(\theta^t) + \lambda g(\theta^t), \quad \text{where } \theta^t = (W^t, x^t), p(\theta^t) = g(W^t, x^t) - g(W^t, x_t^*) \\
 \nabla f(W, x) &= (\nabla_W f(W, x), \nabla_x f(W, x)), \quad \nabla g(W, x) = (\nabla_W g(W, x), \nabla_x g(W, x)).
 \end{aligned} \tag{7}$$

Lemma 1. *Let (W, x) be a solution to the \mathcal{BP}_ϵ . This point is also an ϵ -accurate Pareto stationarity point for $\{l_i(x)\}$ satisfying*

$$\min_{w \in \mathcal{W}} \|G(x)w\|^2 = \mathcal{O}(\epsilon).$$

Proof. According to the definition of \mathcal{BP}_ϵ , its solution (W, x) satisfies that

$$g(W, x) - g(W, x^*) \leq \epsilon. \tag{8}$$

Algorithm 2 Double-loop First-order method

```

1: Initialize:  $W^0, x^0, z_0^0$ 
2: for  $t = 0, 1, \dots, T - 1$  do
3:   warm start  $z_0^t = x^t$ 
4:   for  $n = 0, 1, \dots, N$  do
5:      $z_{n+1}^t = z_n^t - \beta \lambda \nabla_z g(W^t, z_n^t)$ 
6:   end for
7:    $x^{t+1} = x^t - \alpha (\nabla_x f(W^t, x^t) + \lambda \nabla_x g(W^t, x^t))$ 
8:    $W^{t+1} = W^t - \alpha (\nabla_W f(W^t, x^t) + \lambda (\nabla_W g(W^t, x^t) - \nabla_W g(W^t, z_N^t)))$ 
9: end for

```

Further, according to Assumption 1, we can obtain

$$g(W, x) \geq g(W, x^*) + \nabla_x g(W, x^*)(x - x^*) + \frac{1}{2L_g} \|\nabla_x g(W, x) - \nabla_x g(W, x^*)\|^2.$$

Since $x^* \in \arg \min_x g(W, x)$ and $g(W, x) = \sum_{i=1}^K \sigma_i(W) \tilde{l}_i(x)$, we have $\nabla_x g(W, x^*) = 0$ and $\nabla_x g(W, x) = \sum_{i=1}^K \sigma_i(W) \nabla_x \tilde{l}_i(x) = \tilde{G}(x) \sigma(W)$. We can obtain,

$$\|\tilde{G}(x) \sigma(W)\|^2 \leq 2L_g (g(W, x) - g(W, x^*)) = \mathcal{O}(\epsilon), \quad (9)$$

where the last inequality follows from Equation (8). Furthermore, since we have used softmax at the last layer of our neural network, $\sigma(W)$ belongs to the probability simplex \mathcal{W} . Thus we can derive

$$\min_{w \in \mathcal{W}} \|\tilde{G}(x) w\|^2 \leq \|\tilde{G}(x) \sigma(W)\|^2 = \mathcal{O}(\epsilon).$$

Thus, the solution (W, x) to the \mathcal{BP}_ϵ also satisfies Pareto stationarity of the normalized loss functions $\{\tilde{l}_i\}$. Then we show the equivalence between the Pareto stationarities for the original loss functions $\{l_i\}$ and the normalized loss functions $\{\tilde{l}_i\}$. First, for the identical normalization, the above eq. (9) naturally recovers

$$\min_{w \in \mathcal{W}} \|G(x) w\|^2 = \min_{w \in \mathcal{W}} \|\tilde{G}(x) w\|^2 \leq \|\tilde{G}(x) \sigma(W)\|^2 = \mathcal{O}(\epsilon).$$

Then, for the rescaled normalization, $\tilde{l}_i(x) = \frac{l_i(x)}{l'_i}$ where $\forall i, l'_i = \mathcal{O}(1)$. Thus, we can have

$$\min_{w \in \mathcal{W}} \|G(x) w\|^2 \leq \|G(x) \sigma(W)\|^2 \leq L_{\max}^2 \|\tilde{G}(x) \sigma(W)\|^2 = \mathcal{O}(\epsilon),$$

where $L_{\max} = \max_i l'_i$. Finally, for the logarithmic normalization, $\tilde{l}_i(x) = \log \left(\frac{l_i(x)}{l_{i,0}} \right) = \lim_{\kappa \rightarrow 1} \frac{\left(\frac{l_i(x)}{l_{i,0}} \right)^{1-\kappa} - 1}{1-\kappa}$.

Furthermore, according to the Proposition 6.1 in Ban & Ji 2024, the Pareto front of the $(\tilde{l}_1(x), \tilde{l}_2(x), \dots, \tilde{l}_K(x))$ which can be considered as κ -fair functions is the same as that of loss functions $\left(\frac{l_1(x)}{l_{1,0}}, \frac{l_2(x)}{l_{2,0}}, \dots, \frac{l_K(x)}{l_{K,0}} \right)$. Therefore, for an ϵ -accurate Pareto stationarity point x of the normalized loss functions, we can obtain

$$\min_{w \in \mathcal{W}} \|G'(x) w\|^2 = \mathcal{O}(\epsilon),$$

where $G'(x) = \left(\frac{\nabla l_1(x)}{l_{1,0}}, \frac{\nabla l_2(x)}{l_{2,0}}, \dots, \frac{\nabla l_K(x)}{l_{K,0}} \right)$. Furthermore, we can obtain

$$\min_{w \in \mathcal{W}} \|G(x)w\|^2 \leq \min_{w \in \mathcal{W}} (L'_{\max})^2 \|G'(x)w\|^2 = \mathcal{O}(\epsilon),$$

where $L'_{\max} = \max_i l_{i,0} = \mathcal{O}(1)$. Then with our three normalization approaches, there is an equivalence between the Pareto stationarities of the original loss functions $\{l_i\}$ and the normalized loss functions $\{\tilde{l}_i\}$. The proof is complete. \square

Theorem 2 (Restatement of Theorem 1). *Suppose Assumption 1-Assumption 2 are satisfied. Select hyperparameters*

$$\alpha \in \left(0, \frac{1}{L_f + \lambda(2L_g + L_g^2\mu)}\right], \beta \in \left(0, \frac{1}{L_g}\right], \lambda = L\sqrt{3\mu\epsilon^{-1}}, \text{ and } N = \Omega(\log(\alpha t)).$$

(i) *Our method with the updates eq. (3) and eq. (4) (i.e., Algorithm 2 in the appendix) finds an ϵ -accurate stationary point of the problem \mathcal{BP}_λ . If this stationary point is a local/global solution to \mathcal{BP}_λ , it is also a local/global solution to \mathcal{BP}_ϵ . Furthermore, it is also an ϵ -accurate Pareto stationary point for loss functions $l_i(x), i = 1, \dots, K$.*

(ii) *Moreover, if $\|\nabla_W g(W^t, z_N^t)\| = \mathcal{O}(\epsilon)$ for $t = 1, \dots, T$. The simplified method in Algorithm 1 also achieves the same convergence guarantee as that in (i) with $\mathcal{O}(\epsilon^{-2})$ iterations.*

Proof. We start with the first half of our theorem. Directly from Theorem 3 in Shen & Chen 2023, Algorithm 2 achieves an ϵ -accurate stationary point of \mathcal{BP}_λ with $\tilde{\mathcal{O}}(\epsilon^{-1.5})$ iterations such that

$$\frac{1}{T} \sum_{t=0}^{T-1} \|\nabla f(W^t, x^t) + \lambda(\nabla g(W^t, x^t) - \nabla g(W^t, x_t^*))\|^2 \leq \frac{F(W^0, x^0)}{\alpha T} + \frac{10L^2L_g^2}{T} = \mathcal{O}(\epsilon).$$

Recall that $F(W^0, x^0) = f(W^0, x^0) + \lambda(g(W^0, x^0) - g(W^0, x_0^*))$. According to the Proposition 2 in Shen & Chen 2023 by setting $\delta = \epsilon$ therein, we can have $g(W^T, x^T) - g(W^T, x_T^*) \leq \epsilon$ if this stationary point is local/global solution to \mathcal{BP}_λ . Then by using Lemma 1, we know that this ϵ -accurate stationary point is also an ϵ -accurate Pareto stationary point of normalized functions $\{\tilde{l}_i(x)\}$ satisfying

$$\min_{w \in \mathcal{W}} \|G(x^T)w\|^2 = \mathcal{O}(\epsilon).$$

The proof of the first half of our theorem is complete.

Then for the second half, since we have built the connection between the stationarity of \mathcal{BP}_λ and Pareto stationarity, we prove that the single-loop Algorithm 1 achieves an ϵ -accurate stationary point of \mathcal{BP}_λ . Recall that

$$\begin{aligned} & \|\nabla f(W^t, x^t) + \lambda(\nabla g(W^t, x^t) - \nabla g(W^t, x_t^*))\|^2 \\ & \stackrel{(i)}{\leq} 2\|\nabla f(W^t, x^t) + \lambda\nabla g(W^t, x^t)\|^2 + 2\lambda^2\|\nabla g(W^t, x_t^*)\|^2 \\ & \stackrel{(ii)}{\leq} 2\|\nabla f(W^t, x^t) + \lambda\nabla g(W^t, x^t)\|^2 + 2\lambda^2\|\nabla_W g(W^t, x_t^*)\|^2 \\ & \stackrel{(iii)}{\leq} 2\|\nabla f(W^t, x^t) + \lambda\nabla g(W^t, x^t)\|^2 + 4\lambda^2\|\nabla_W g(W^t, x_t^*) - \nabla_W g(W^t, z_N^t)\|^2 + 4\lambda^2\|\nabla_W g(W^t, z_N^t)\|^2, \end{aligned} \tag{10}$$

where (i) and (iii) both follow from Young's inequality, and (ii) follows from $\nabla_x g(W^t, x_t^*) = 0$. Besides, recall that z_N^t is the intermediate output of the subloop in Algorithm 2. We next provide the upper bounds of the above three terms on the right-hand side (RHS). For the first term, we utilize the smoothness of $\Phi(\theta^t) = f(\theta^t) + \lambda g(\theta^t)$ where $L_\Phi = L_f + \lambda L_g$ and $\theta^t = (W^t, x^t)$.

$$\begin{aligned}\Phi(\theta^{t+1}) &\leq \Phi(\theta^t) + \langle \nabla \Phi(\theta^t), \theta^{t+1} - \theta^t \rangle + \frac{L_\Phi}{2} \|\theta^{t+1} - \theta^t\|^2 \\ &\stackrel{(i)}{\leq} \Phi(\theta^t) - \frac{\alpha}{2} \|\nabla \Phi(\theta^t)\|^2,\end{aligned}$$

where (i) follows from $\alpha \leq \frac{1}{L_\Phi} = \mathcal{O}(\lambda^{-1})$. Thus, we can obtain

$$\|\nabla \Phi(\theta^t)\|^2 \leq \frac{2}{\alpha} (\Phi(\theta^t) - \Phi(\theta^{t+1})). \quad (11)$$

Then for the second term on the RHS in eq. (10), we follow the same step in the proof of Theorem 3 in Shen & Chen 2023 and obtain

$$\begin{aligned}4\lambda^2 \|\nabla_W g(W^t, x_t^*) - \nabla_W g(W^t, z_N^t)\|^2 &\leq 4\lambda^2 L_g^2 \mu \left(1 - \frac{\beta}{2\mu}\right)^N (g(W^t, x^t) - g(W^t, x_t^*)) \\ &\stackrel{(i)}{\leq} 4\lambda^2 L_g^2 \left(1 - \frac{\beta}{2\mu}\right)^N \|\nabla_x g(W^t, x^t)\|^2 \\ &= 4\lambda^2 L_g^2 \left(1 - \frac{\beta}{2\mu}\right)^N \left\| \frac{x^{t+1} - x^t + \alpha \nabla_x f(W^t, x^t)}{\alpha \lambda} \right\|^2 \\ &\stackrel{(ii)}{\leq} 8\lambda^2 L_g^2 \left(1 - \frac{\beta}{2\mu}\right)^N \left(\frac{\|\theta^{t+1} - \theta^t\|^2}{\alpha^2 \lambda^2} + \frac{L^2}{\lambda^2} \right) \\ &\stackrel{(iii)}{\leq} \frac{1}{2\alpha^2} \|\theta^{t+1} - \theta^t\|^2 + \frac{2L^2 L_g^2}{\alpha^2 t^2} \\ &= \frac{1}{2} \|\nabla \Phi(\theta^t)\|^2 + \frac{2L^2 L_g^2}{\alpha^2 t^2},\end{aligned} \quad (12)$$

where (i) follows from the PL condition, (ii) follows from Young's inequality and Assumption 1, and (iii) follows from the selection on $N \geq \max\{-\log_{c_\beta}(16L_g^2), -2\log_{c_\beta}(2\alpha t)\}$ with $c_\beta = 1 - \frac{\beta}{2\mu}$. Lastly, for the last term at the RHS in eq. (10), we have,

$$4\lambda^2 \|\nabla_W g(W^t, z_N^t)\|^2 = \mathcal{O}(\lambda^2 \epsilon^2), \quad (13)$$

where this inequality follows from our experimental observation. Furthermore, substituting eq. (11), and eq. (12) into eq. (10) yields

$$\begin{aligned}\|\nabla f(W^t, x^t) + \lambda(\nabla g(W^t, x^t) - \nabla g(W^t, x_t^*))\|^2 &\leq \frac{5}{2} \|\nabla \Phi(\theta^t)\|^2 + \frac{2L^2 L_g^2}{\alpha^2 t^2} + 4\lambda^2 \|\nabla_W g(W^t, z_N^t)\|^2 \\ &\leq \frac{5}{\alpha} (\Phi(\theta^t) - \Phi(\theta^{t+1})) + \frac{2L^2 L_g^2}{\alpha^2 t^2} + 4\lambda^2 \|\nabla_W g(W^t, z_N^t)\|^2.\end{aligned} \quad (14)$$

Therefore, telescoping the above inequality yields,

$$\begin{aligned} & \frac{1}{T} \sum_{t=0}^{T-1} \|\nabla f(W^t, x^t) + \lambda(\nabla g(W^t, x^t) - \nabla g(W^t, x_t^*))\|^2 \\ &= \mathcal{O}\left(\frac{\lambda}{\alpha T} + \frac{1}{\alpha^2 T} + \lambda^2 \epsilon^2\right). \end{aligned}$$

According to the parameter selection that $\lambda = \mathcal{O}(\epsilon^{-\frac{1}{2}})$, $\alpha = \mathcal{O}(\epsilon^{\frac{1}{2}})$, and $T = \Omega(\epsilon^{-2})$, we can obtain

$$\frac{1}{T} \sum_{t=0}^{T-1} \|\nabla f(W^t, x^t) + \lambda(\nabla g(W^t, x^t) - \nabla g(W^t, x_t^*))\|^2 = \mathcal{O}(\epsilon).$$

Therefore, Algorithm 1 can achieve a stationary point of \mathcal{BP}_λ with $\mathcal{O}(\epsilon^{-2})$ iterations. If this stationary point is a local/global solution to \mathcal{BP}_λ , it is also a solution to \mathcal{BP}_ϵ according to Proposition 2 in Shen & Chen 2023. Then by using Lemma 1, we know this stationary point is also an ϵ -accurate Pareto stationary point of the original loss functions. The proof is complete. \square